Supporting Information:

Photo and Electronic Excitation for Low Temperature Catalysis over Metal Nanoparticles via Organic Semiconductor

Weiran Zheng[1,2], Simon Jones[1], Xinlin Hong[2], Shik Chi Edman Tsang[1*]

[1] *Wolfson Catalysis Centre, Department of Chemistry, University of Oxford, Oxford, OX1 3QR, UK*

[2] *College of Chemistry and Molecular Sciences, Wuhan University, Wuhan 430072, PRC*

1 TEM Characterization:

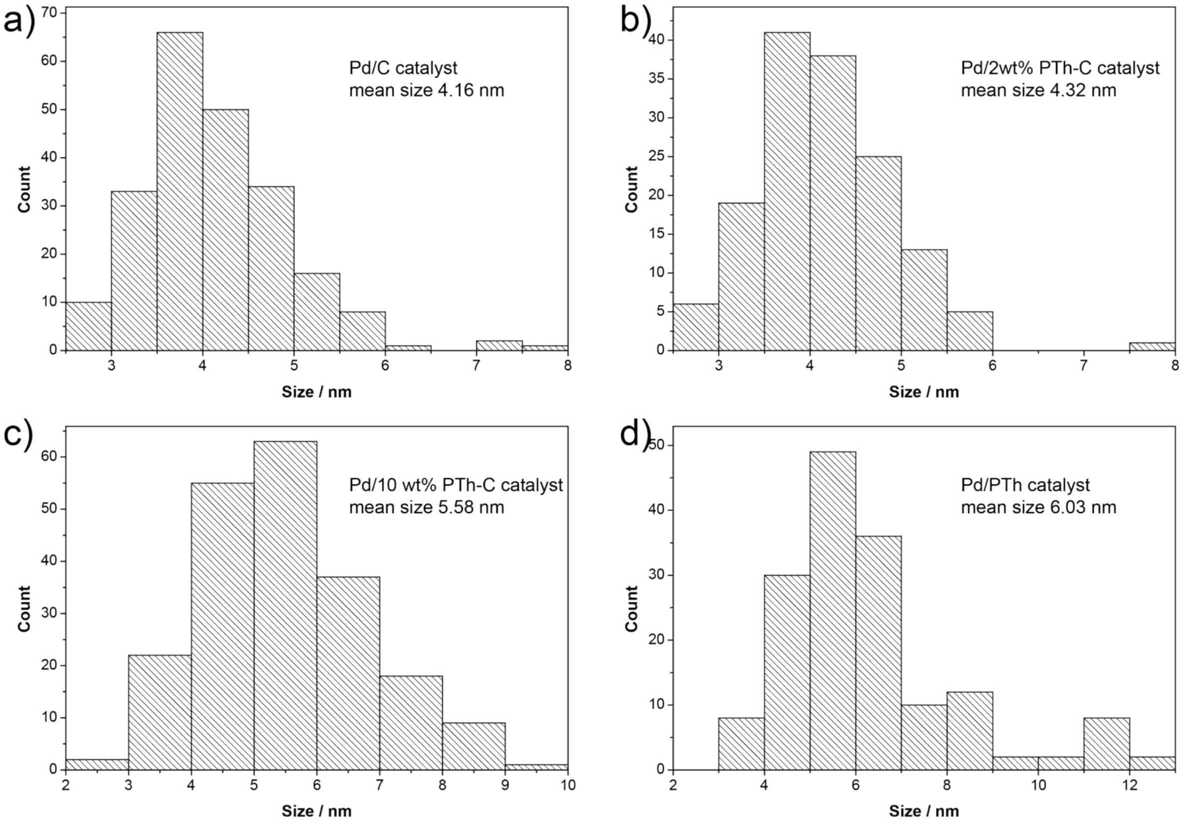

Figure S1 Pd nanoparticle size distribution counted from TEM images. ***a*** *Pd/C catalyst,* ***b*** *Pd/2wt% PTh-C catalyst,* ***c*** *Pd/10 wt% PTh-C catalyst and* ***d*** *Pd/PTh catalyst.*

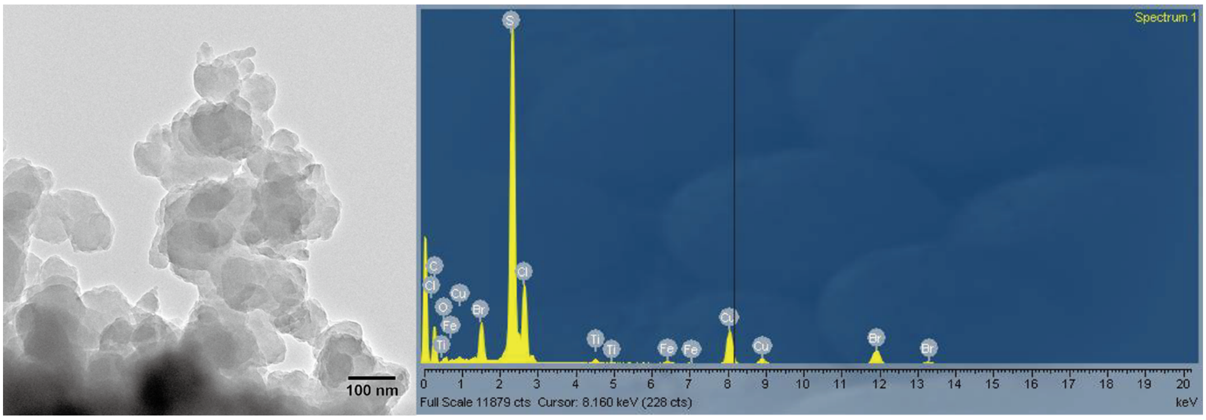

Figure S2-1 TEM image of polythiophene nanoparticles together with selected EDX spectrum.

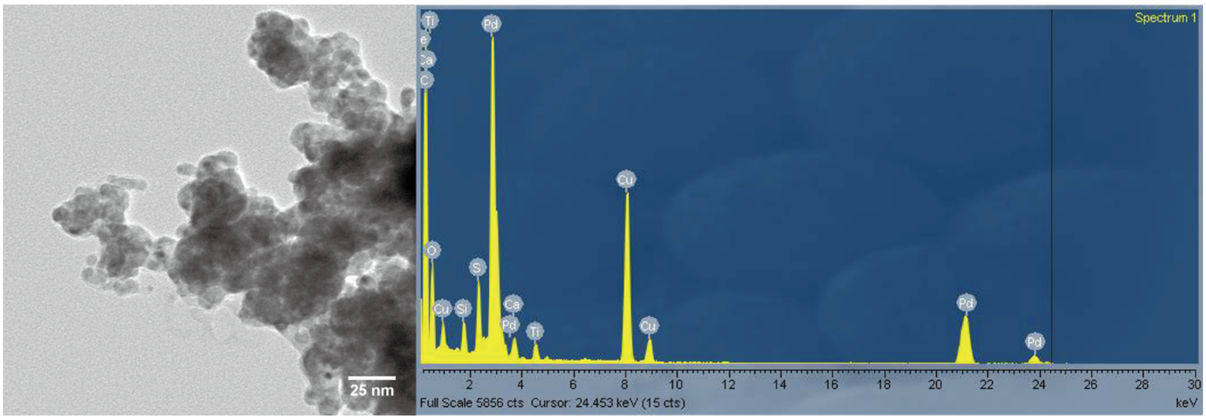

Figure S2-2 TEM image of 10wt% Pd/polythiophene nanoparticles together with selected EDX spectrum.

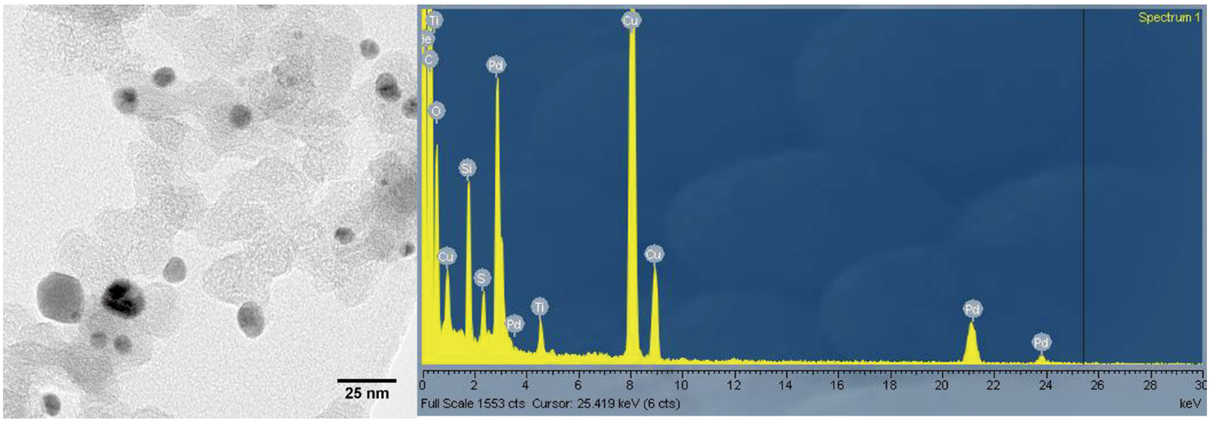

Figure S2-3 TEM image of 10wt% Pd/20% PTh-C nanoparticles together with selected EDX spectrum.

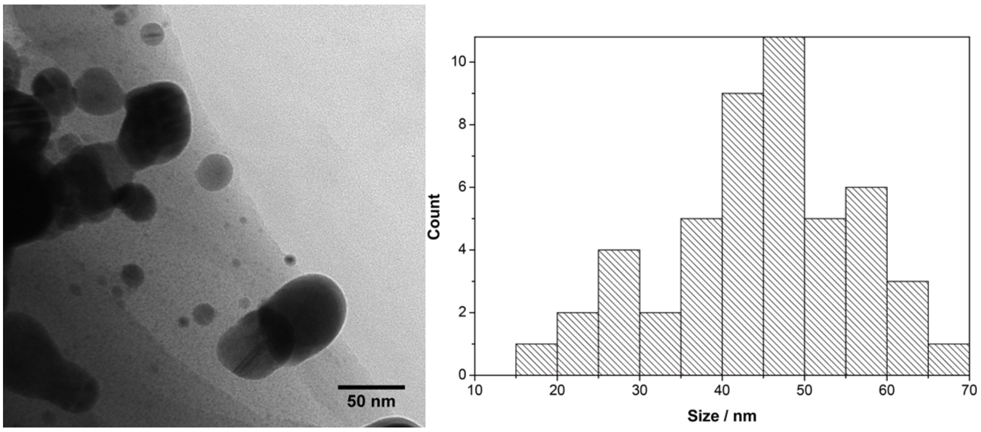

Figure S3 TEM image of 10 wt% Ag/PTh nanoparticles.

2 Kubelka-Munk equation[S1]:

$$F(R)=(1-R^2)/2R=k/s$$

R=absolute reflectance of the layer

k=molar absorption coefficient

s=scattering coefficient

3 Raman Spectroscopy:

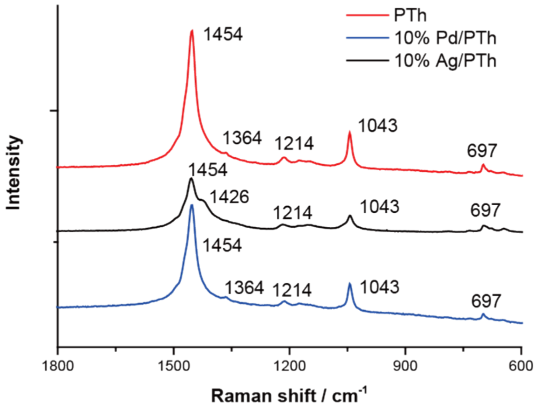

Figure S4 Raman spectra of polythiophene and polythiophene loaded with 10 wt% metal together with assignment of the Raman bands, see Table S1. New peak shown at 1426 cm^{-1} in 10wt% Ag/PTh comparing to PTh and 10wt% Pd/PTh indicating the electron acceptance of conjugated C=C rings from excited Ag at room temperature[S2].

Table S1 Assignment of vibrational modes[S2].

v / cm^{-1}	Assignment of vibrational modes
1454	C_α=C_β symmetric stretching
1364	C_β–C_α’ stretching
1214	C_α–C_α’ interring stretching
1043	C_β’-H bending
697	C–S–C deformation

4 Electro-analytical Characterization:

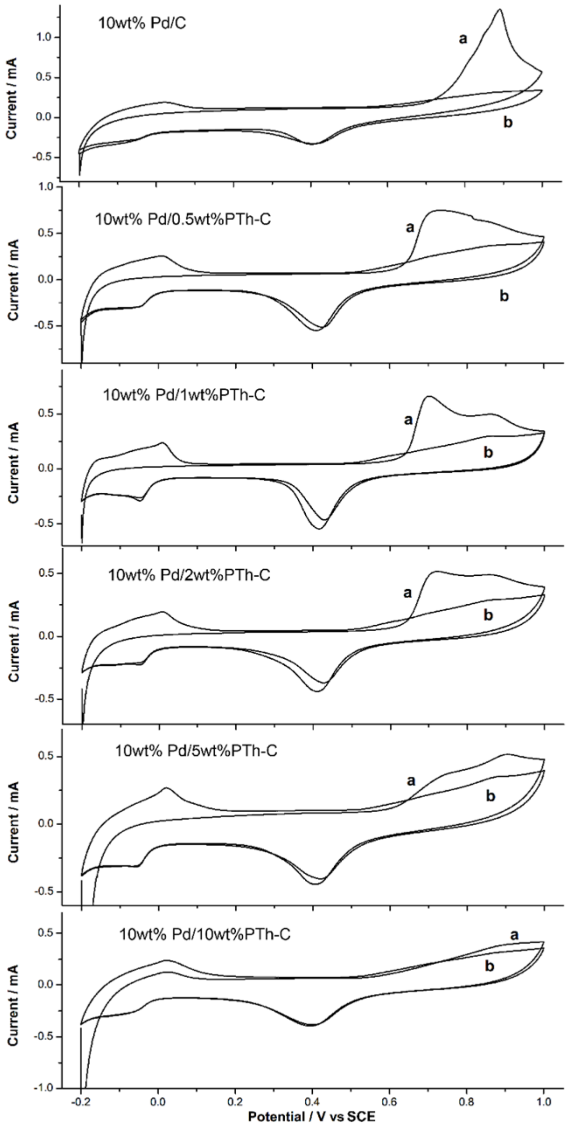

*Figure S5 CO_{ads} stripping voltammograms at 10 wt.% Pd catalysts with different supports in 0.5 mol/L H_2SO_4 after exposed to saturated CO at 0.2 V and followed by removing residue CO. Line **a** indicated first cycle of CO stripping, and line **b** indicated second cycle of stripping.*

5 $^{12}CO/^{13}CO$ adsorption ATR-FTIR test

$^{12}CO/^{13}CO$ experiment was performed in room temperature and 1 atm. To prepare $^{12}CO/^{13}CO$ (ratio of 76/24) covered PVP-Pd sample, excess $H^{12}COOH$ and $H^{13}COOH$ (kept at % molar ratio of 76: 24) was mixed with PVP-Pd colloid then heated up to 100°C to produce corresponding adsorbed ^{12}CO and ^{13}CO on metal surface until no further gas was formed indicative of a full CO coverage of Pd sites. The solution was then applied and dried on the ATR crystal under N_2 and room temperature.

$$HCOOH \xrightarrow{\text{high temperature}} CO + H_2O$$

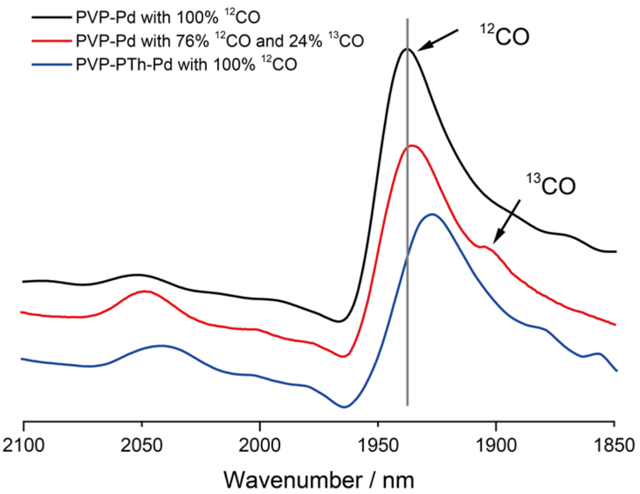

Figure S6 It is noted from the CO adsorptions of the spectra of PVP-Pd (100% ^{12}CO) and PVP-PTh-Pd (100% ^{12}CO), the decrease in Pd surface area caused by PTh was estimated to be 24% by comparing their integrated CO bridge peaks. As a result, 76:24 of ^{12}CO/^{13}CO adsorption spectra were collected over PVP-Pd using corresponding ratio H^{12}COOH and H^{13}COOH, followed by their decomposition on the Pd surface. A red shift of 4 cm^{-1} of ^{12}CO is obtained (^{13}CO at 1903 cm^{-1}) as compared to the red shift of 11cm^{-1} of ^{12}CO PVP-PTh-Pd at the equivalent coverage.

6 XPS Characterization:

Sample characterizations by X-ray photoelectron spectroscopy[S3] were carried out and are shown in Figure S7. The spectra of polythiophene were also collected and used as a standard for comparison (Figure S7-1). With the introduction of Pd, two pairs of spin-orbital coupling peaks of Pd can be clearly seen. The binding energy peaks of $Pd^{II}3d_{5/2}$ and $Pd^{II}3d_{3/2}$ (338.13eV and 343.33 eV) are attributed to the Pd(II) directly bonded to S atom of polythiophene. The lower binding energy peaks of $Pd^{0}3d_{5/2}$ and $Pd^{0}3d_{3/2}$ (336.12eV and 341.32eV) correspond to Pd nanoparticles without the direct contact of polythiophene presumably the particles are buried deep in the porous carbon structure (refer to CO stripping experiments). Also, it is found that there are two C1s signals shown according to XPS spectrum, one could be attributed to amorphous carbon (285.10 eV) and the other to the C atoms from polythiophene (286.85 eV). The value of $S2p_{3/2}$ peak is in a good agreement with literature value of thiophene compound with reference to the C1s. In the case of Ag/PTh, only one pair of spin-orbital coupling peaks of Ag are observed due to the fact that the synthesised Ag particles were considerably larger than Pd without much ultrafine Ag nanoparticles within the porous carbon.

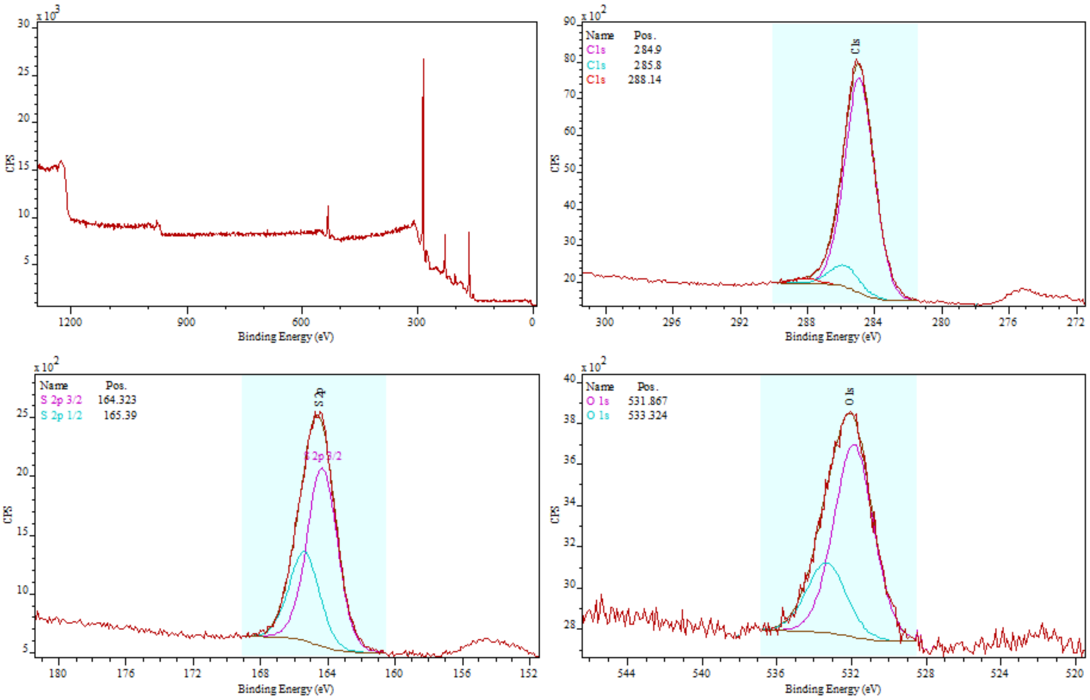

Figure S7-1 XPS spectra of polythiophene: 77.3 at% C; 6.7 at% O; 16 at% S.

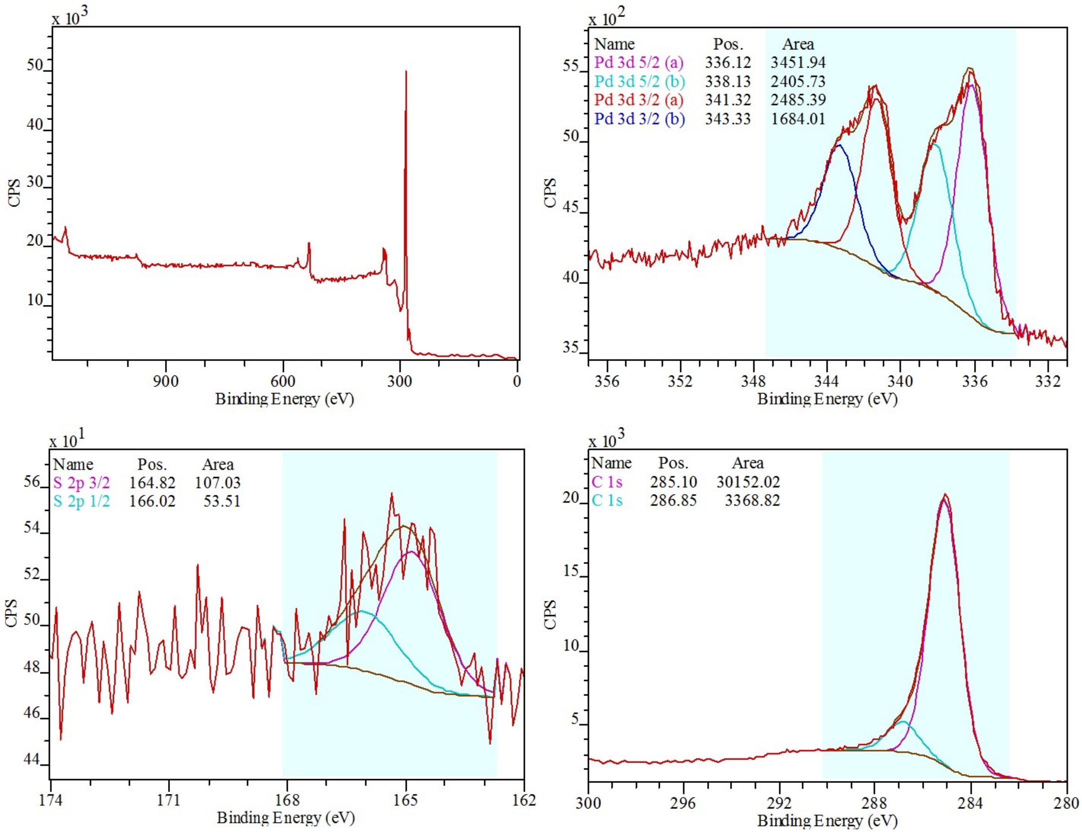

Figure S7-2 XPS spectra of 10 wt% Pd/2wt% PTh-C: 1.7at% Pd; 0.3 at% S; 6.9 at% O; 91.1 at% C.

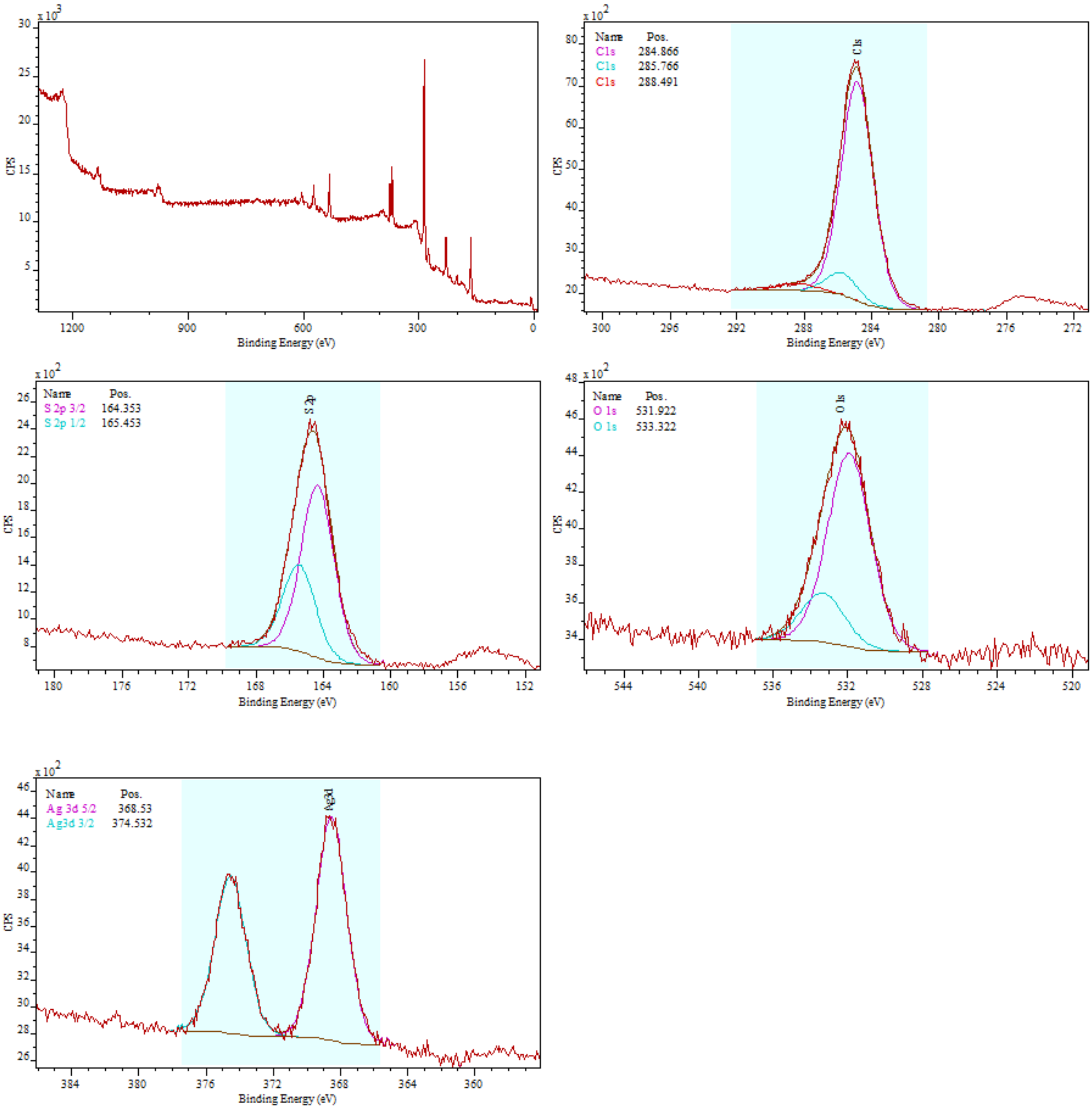

Figure S7-3 XPS spectra of Ag/polythiophene: 76.4 at% C; 6.9 at% O; 14.7 at% S; 2 at% Ag.

7 Catalytic Testing:

Table S2 Catalytic activities for formic acid decomposition over various catalysts with and without light illumination

10%M/C Catalysts	Metal Surface Area (m^2/g)	Temp	H_2/CO_2 ratio	Initial act. In dark ($mmol_{gas}\ h^{-1}m^{-2}_{Pd}$)	Initial act. In light ($mmol_{gas}\ h^{-1}m^{-2}_{Pd}$)
Pd	5.36	25	1.01	2.59	2.57
Pd/ 0.5% PTh	6.99	25	0.99	2.73	6.32
Pd/ 1% PTh	4.46	25	1.00	6.48	14.1
Pd/ 2% PTh	4.37	25	0.99	8.48	17.5
Pd/ 5% PTh	3.58	25	1.00	3.88	7.65
Pd/10% PTh	2.59	25	1.02	1.69	3.31
Pd/20% PTh	1.09	25	1.01	1.50	2.74
AgPd	6.92	25	1.02	32.7	31.6
AgPd	6.92	40	0.99	71.0	68.4
AgPd	6.92	60	0.99	98.4	92.3
AgPd/2% PTh	4.97	25	1.01	39.6	42.3
AgPd/2% PTh	4.97	40	0.98	98.7	122.3

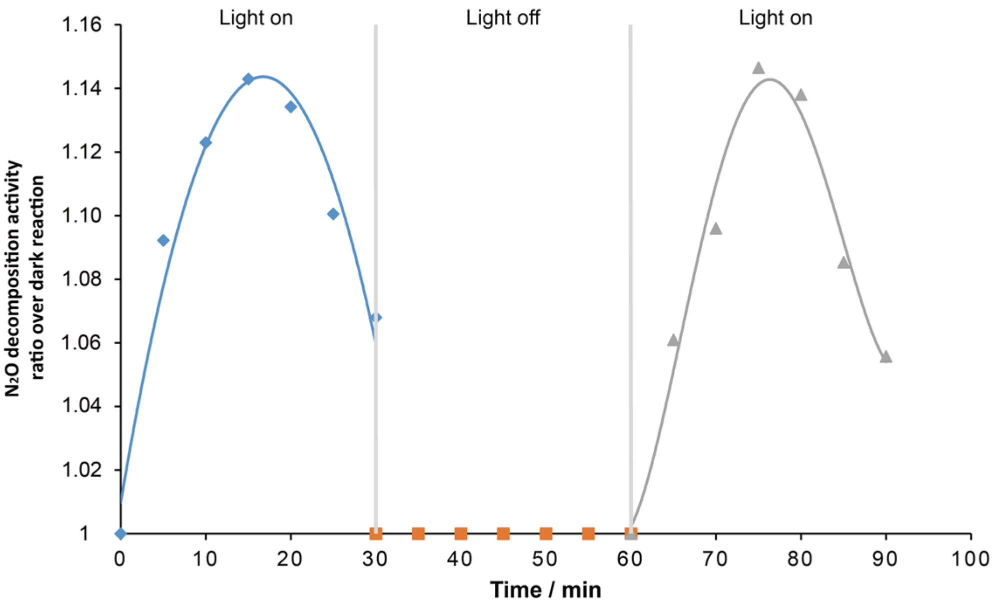

Figure S8 Cyclic N_2O decomposition activity ratio (conversion under light/conversion under dark) over 50 mg Pd/2wt%PTh/C, 0.3 atm, with 2500 ppm N_2O, 4.75% Ar in 95% H_2 at RT; light and dark period 30 min each.

Light source: The UV lamp used for this work was supplied by Helios Italquartz, 500 Watts. The UV range below 430 nm was deliberately blocked by a longpass filter (type LP 430) from Schneider Kreuznach. An experiment was carried out to evaluate the effect of UV range on catalytic reactions, the light with and without UV radiation did not seem to affect the electron promotion effect of polymer by the visible light, see figure S9.

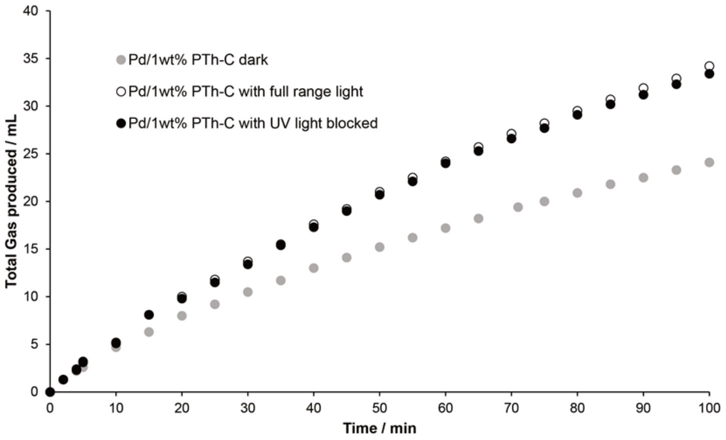

Figure S9 Formic acid decomposition by light irradiation with and without blocking the UV region, experiment was performed at RT.

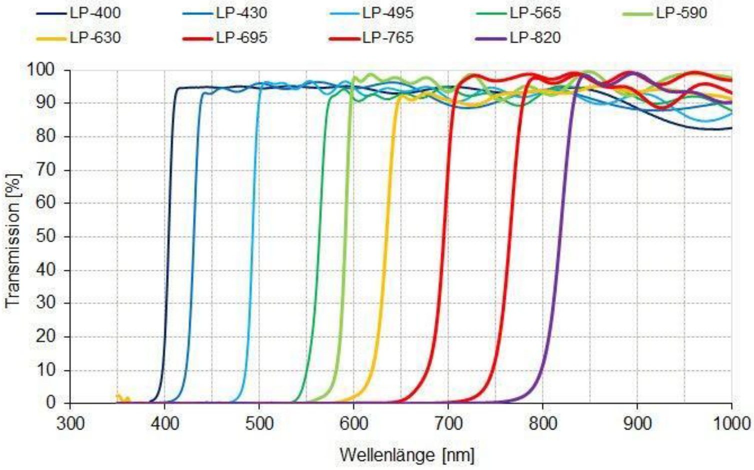

Figure S10 Technical detail of the longpass filter provided by Schneider Kreuznach, copyright © 04/2012 Jos. Schneider Optische Werke GmbH.

Reference

S1. Tauc, J., Grigorovici, R. & Vancu, a. Optical Properties and Electronic Structure of Amorphous Germanium. *Phys. Status Solidi* **15,** 627–637 (1966).

S2. Shi, G., Xu, J. & Fu, M. Raman spectroscopic and electrochemical studies on the doping level changes of polythiophene films during their electrochemical growth processes. *J. Phys. Chem. B* **106,** 288–292 (2002).

S3. *NIST X-ray Photoelectron Spectroscopy (XPS) Database*.